Biological Psychiatry: CNNI

Archival Report

Mapping Disease Course Across the Mood Disorder Spectrum Through a Research Domain Criteria Framework

Alexis E. Whitton, Poornima Kumar, Michael T. Treadway, Ashleigh V. Rutherford, Manon L. Ironside, Dan Foti, Garrett Fitzmaurice, Fei Du, and Diego A. Pizzagalli

ABSTRACT

BACKGROUND: The National Institute of Mental Health Research Domain Criteria (RDoC) initiative aims to establish a neurobiologically valid framework for classifying mental illness. Here, we examined whether the RDoC construct of reward learning and three aspects of its underlying neurocircuitry predicted symptom trajectories in individuals with mood pathology.

METHODS: Aligning with the RDoC approach, we recruited individuals (n = 80 with mood disorders [58 unipolar and 22 bipolar] and n = 32 control subjects; 63.4% female) based on their performance on a laboratory-based reward learning task rather than clinical diagnosis. We then assessed 1) anterior cingulate cortex prediction errors using electroencephalography, 2) striatal reward prediction errors using functional magnetic resonance imaging, and 3) medial prefrontal cortex glutamatergic function (mPFC Gln/Glu) using ^{1}H magnetic resonance spectroscopy. Severity of anhedonia, (hypo)mania, and impulsivity were measured at baseline, 3 months, and 6 months.

RESULTS: Greater homogeneity in aspects of brain function (mPFC Gln/Glu) was observed when individuals were classified according to reward learning ability rather than diagnosis. Furthermore, mPFC Gln/Glu levels predicted more severe (hypo)manic symptoms cross-sectionally, predicted worsening (hypo)manic symptoms longitudinally, and explained greater variance in future (hypo)manic symptoms than diagnostic information. However, rather than being transdiagnostic, this effect was specific to individuals with bipolar disorder. Prediction error indices were unrelated to symptom severity.

CONCLUSIONS: Although findings are preliminary and require replication, they suggest that heightened mPFC Gln/Glu warrants further consideration as a predictor of future (hypo)mania. Importantly, this work highlights the value of an RDoC approach that works in tandem with, rather than independent of, traditional diagnostic frameworks.

https://doi.org/10.1016/j.bpsc.2021.01.004

The Diagnostic and Statistical Manual of Mental Disorders (DSM) (1) and International Classification of Diseases (2) classify major depressive disorder (MDD) and bipolar disorder (BD) as separate conditions distinguishable by a history of (hypo)mania, with evidence supporting a disease-specific treatment approach (3,4). Although these nosological systems provide a useful common language for clinicians and researchers, their value for understanding mood disorder pathophysiology remains limited. Accordingly, the Research Domain Criteria (RDoC) (5,6) was proposed as a strategic change in scientific inquiry and seeks to classify psychiatric disorders according to measurable variability within and across different domains of functioning. Subsequently, the Positive Valence Systems domain—in particular, the subdomain of reward learning—has emerged as an especially promising target for understanding the mechanisms underpinning mood symptoms.

Reward learning refers to the ability to adaptively modulate behavior as a function of positive reinforcement. Abnormalities in reward learning and underlying neurocircuitry have been strongly implicated in mood disorders (7,8). For example, performance on behavioral reward learning paradigms has been shown to 1) differentiate patients with MDD or BD from control subjects during symptomatic and asymptomatic states (9,10), 2) predict anhedonia severity and treatment outcome (11), 3) change following pharmacological dopaminergic manipulations (12,13), 4) be linked to striatal dopamine transporter function and frontostriatal functional connectivity (14), and 5) be heritable (15). Decades of research in laboratory animals has identified the neurobiological processes underpinning reward learning (16). Therefore, examining how these processes vary across the mood disorder spectrum represents a fruitful avenue for identifying the neurobiological basis underpinning mood disorder heterogeneity.

Imaging and computational studies suggest that the brain employs distinct hierarchical systems to support learning (17,18), and to date the neural circuitry involved in learning from positive reinforcement has been especially well characterized (19–21). Importantly, individuals with MDD or BD have

 ISSN: 2451-9022

been found to exhibit dysregulation in three key aspects of this neurocircuitry. First, a fundamental mechanism that supports reward learning is the reward prediction error (RPE), which is a striatal dopamine-based signal that encodes violations of reward expectancies (22). Individuals with MDD have been found to have blunted striatal RPE signals during learning (23–25), and this blunting has been linked to a more recurrent depressive illness course (23). Similar abnormalities have been observed in individuals with BD, although the direction of effects often diverges from those observed in studies of unipolar MDD. Relative to healthy control subjects, euthymic individuals with BD or individuals with subthreshold hypomania have been found to have elevated striatal activation during reward anticipation (26) and reward outcome (27). Similarly, manic individuals with BD show striatal responses that fail to differentiate between receipt and omission of rewards, suggestive of abnormal RPE signaling (28).

Second, event-related potential (ERP) studies highlight the reward positivity (RewP) as another important reward circuit component linked to mood pathology (29). The RewP is a frontocentral electroencephalographic (EEG) deflection that is elicited by RPEs and is thought to originate from the anterior cingulate cortex (ACC) and striatum (30). Smaller RewP amplitudes, as well as weaker RewP-related ACC activation, predict poorer reward learning (31,32). Furthermore, abnormal RewP amplitudes have been observed in individuals with hypomania (33) and those with MDD (34), and they have been found to predict future depression onset in healthy individuals (35). Critically, the source of these RewP signals is believed to be distinct from that of striatal dopaminergic RPEs (36); hence, they offer complementary information to functional magnetic resonance imaging (fMRI)-based RPE studies in terms of understanding the biological basis of reward learning dysfunction.

Finally, while the reward learning literature has historically emphasized the role of dopamine, the hedonic effects of dopamine are thought to be partially mediated by its interactions with glutamatergic signals originating in the medial prefrontal cortex (mPFC) (37). In line with this notion, in animal studies disrupted glutamate signaling between mPFC and striatal regions impairs reward motivation (38), and in psychiatrically healthy humans mPFC glutamate levels (measured using magnetic resonance spectroscopy [MRS]) predict reward-based decision making (39). Human MRS studies often focus on the glutamine/glutamate ratio (Gln/Glu) because glutamate is released into the synaptic cleft, taken up by glial cells, converted into glutamine, and cycled back into neurons (40), making mPFC Gln/Glu a proxy measure of the integrity of the glutamatergic synapse. Of note, meta-analyses of MRS studies have highlighted mPFC glutamate abnormalities in MDD and BD, albeit in opposite directions, with glutamatergic transmission being reduced in MDD (41) but elevated in BD (42) across manic (43), depressive (44), and euthymic (45) mood states.

Taken together, these studies suggest that striatal and ACC-mediated PE signals, along with mPFC Gln/Glu, are promising biomarkers of reward learning that may be implicated in mood pathology. Therefore, the aim of this study was to determine whether variation in reward learning neurocircuit function predicts variability in symptom trajectories in individuals with mood disorders. In line with the grant mechanism supporting this study (RFA-MH-14-050; Dimensional Approaches to Research Classification in Psychiatric Disorders), we recruited individuals based on their performance on a well-validated behavioral reward learning task rather than on the basis of specific DSM diagnoses. We then examined whether neurobiological indices of reward learning predicted cross-sectional and longitudinal variation in three reward-relevant symptom domains, namely anhedonia, (hypo)mania, and impulsivity. We predicted that potentiated striatal and ACC-mediated PEs, and elevated mPFC Gln/Glu, would predict worsening (hypo)mania and impulsivity. In contrast, we predicted that blunted striatal and ACC-mediated PEs, and reduced mPFC Gln/Glu, would predict worsening anhedonia. Importantly, we assessed whether these reward learning biomarkers provided superior predictive validity in determining symptom trajectories relative to clinical diagnostic information alone.

METHODS AND MATERIALS

Participants

Subjects in the mood pathology group were required to have depressive, mixed, or hypomanic symptoms severe enough to cause distress/impairment. Participants could pursue treatment but were excluded from further testing if they initiated one of the exclusionary treatments (see Supplemental Methods). Psychotropic medication load was quantified using previously established procedures (Supplemental Methods). Subjects in the control group had no lifetime psychiatric disorders or psychotropic medication use. This study was approved by the Partners Human Research Committee. Participants provided written informed consent prior to participating.

Study Design and Recruitment

Figure 1A shows the study design. Recruitment occurred as follows. Healthy control subjects and treatment-seeking individuals with mood disorders were screened on a probabilistic reward task (PRT) (10,46). Screening continued until two conditions were met: 1) a sample of 32 healthy control subjects with valid PRT data, and who met study eligibility criteria, was recruited and 2) a sample of 80 individuals with mood pathology whose PRT performance spanned the full range of a normative distribution, and who met study eligibility criteria, was recruited. For the 80 individuals with mood pathology, we focused on equally populating quintiles of reward learning ($n \sim$ 16/quintile) (Figure 2) that were defined using cutoffs derived from a prior normative sample of 572 control subjects who had performed the PRT in prior studies. In total, 272 individuals needed to be screened on the PRT to reach these two criteria (see Figure S1 for study flow diagram).

For participants who were screened on the PRT and had valid data, study eligibility criteria and clinical diagnoses were further evaluated via a Structured Clinical Interview for DSM-IV (47) conducted by master's- or Ph.D.-level interviewers. Participants were also screened with the Young Mania Rating Scale (48) to ensure that at least one third of the mood pathology sample exhibited (hypo)manic symptoms. Eligible

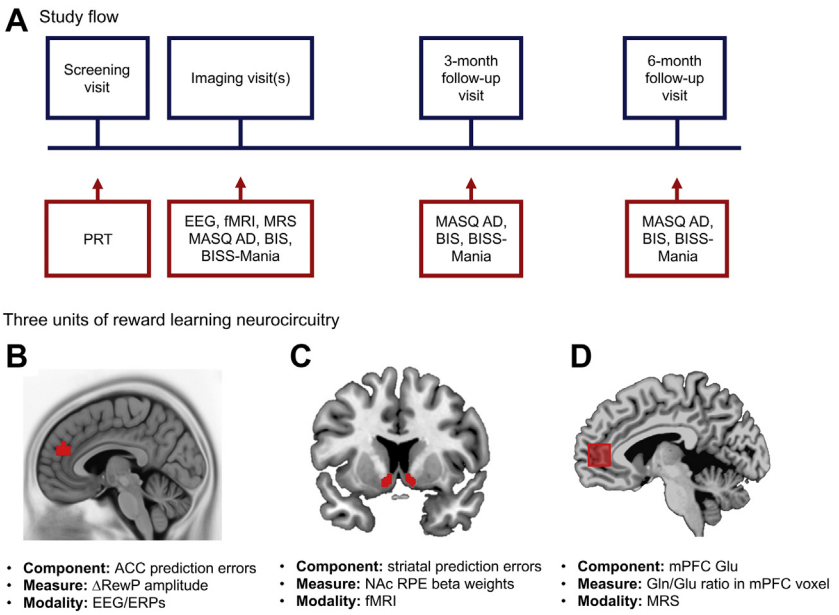

Figure 1. Study methods overview. **(A)** Summary of the study flow. Participants were screened on a probabilistic reward task (PRT), and the patient group was recruited so that patients' scores on the PRT spanned the entire range of possible scores on a preexisting normative distribution. If eligible, a clinical assessment was conducted and then participants returned for two baseline neuroimaging visits (electroencephalography [EEG] and functional magnetic resonance imaging [fMRI]/magnetic resonance spectroscopy [MRS] sessions) as well as 3- and 6-month follow-up assessments. **(B)** Source localization analyses demonstrated that scalp-recorded reward positivity (RewP) amplitude correlated with current source density in the dorsal anterior cingulate cortex (ACC) ($p < .005$ uncorrected; x = −3), validating RewP amplitude as a marker of ACC-mediated activation. **(C)** Bilateral nucleus accumbens (NAc) region of interest (y = 10) from which striatal reward prediction errors (RPEs) were extracted. **(D)** The 2 × 2 × 2-cm voxel placed in the medial prefrontal cortex (mPFC) (x = 0) from which glutamine/glutamate (Gln/Glu) metabolites were extracted. BIS, Barratt Impulsiveness Scale; BISS-Mania, Mania subscale of the Bipolar Inventory of Symptoms Scale; ERP, event-related potential; MASQ AD, Anhedonic Depression subscale of the Mood and Anxiety Symptom Questionnaire.

participants completed five study visits: 1) behavioral testing and clinical assessment, 2) a baseline EEG/ERP recording, 3) a baseline MRI scan, 4) a 3-month follow-up clinical assessment, and 5) a 6-month follow-up clinical assessment. Participants received $15/hour in compensation plus earnings on the behavioral and imaging tasks.

Primary Outcomes

Anhedonia was measured using the Anhedonic Depression subscale of the 62-item Mood and Anxiety Symptom Questionnaire (MASQ-AD) (49), and impulsivity was assessed using the Barratt Impulsiveness Scale (BIS) (50). (Hypo)mania was measured using the Mania subscale of the Bipolar Inventory of Symptoms Scale (BISS-mania), which was chosen over the Young Mania Rating Scale because it measures an extended range of (hypo)manic symptoms (51) and showed greater variance across both unipolar and bipolar groups. These measures were completed at baseline and again at 3- and 6-month follow-up assessments. All three scales demonstrated good internal consistency (Supplemental Methods).

PRT: Quantifying Reward Learning

Reward learning was assessed using a well-validated computer-based PRT (46). On each trial, a fixation cross (500 ms) was followed by a schematic mouthless face (500 ms). Next, a short (11.5-mm) or long (13-mm) mouth appeared (100 ms). Participants indicated whether the mouth was long or short. There were 3 blocks of 100 trials, and for each block 40 correct trials were rewarded ("Correct!! You won 20 cents"). Although long and short mouths were presented at equal frequency,

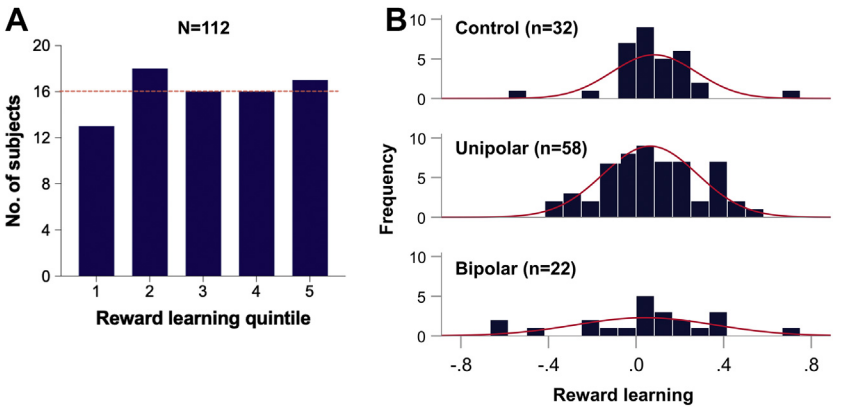

Figure 2. Recruitment based on behavioral reward learning. **(A)** Number of participants with mood pathology whose probabilistic reward task performance fell in each quintile of reward learning performance according to the normative distribution. (The normative distribution was based on a separate existing sample of $N = 572$ healthy control subjects.) The dotted line indicates the a priori target of $n = 16$ per quintile that was set to ensure that we recruited individuals who spanned the entire range of reward learning performance. This target was met in all but the lowest quintile; however, this quintile was still adequately represented with a sample of $n = 13$. **(B)** Frequency histograms of reward learning performance across the control, unipolar, and bipolar groups.

unbeknownst to participants, correct identification of one mouth (the rich stimulus) was rewarded 3 times more than the other mouth (the lean stimulus).

Following quality control (Supplemental Methods), we used signal detection analysis (52) to compute response bias (the tendency to bias responding to the rich stimulus) using the following formula:

$$\log b = \frac{1}{2} \log\left(\frac{Rich_{\text{correct}} \times Lean_{\text{incorrect}}}{Rich_{\text{incorrect}} \times Lean_{\text{correct}}}\right)$$

To allow calculation of response bias for cases that included a zero in the formula, 0.5 was added to each cell of the matrix (53). Reward learning was defined as the increase in response bias from block 1 to block 3.

Scalp-Recorded RewP Amplitude: Quantifying ACC PEs

The RewP was computed from 128-channel scalp-recorded EEG acquired while participants performed a counterbalanced version of the PRT. After preprocessing, temporospatial principal components analysis (PCA) was used to decompose the time domain ERP (54). Temporal variance in the averaged ERP waveforms was examined using temporal PCA and infomax rotation. Based on the scree plot used to determine the factors to retain in a PCA analysis, 12 temporal factors were retained for rotation. The spatial distribution of these temporal factors was then examined using spatial PCA and infomax rotation, with a spatial PCA being conducted for each temporal factor. Eight spatial factors were retained for each temporal factor. Analyses focused on the PCA component with timing and topography most consistent with the RewP (TF8/SF2; see Supplemental Methods). Furthermore, source localization (55) confirmed that the RewP had a source in the dorsal ACC (Figure 1B). Our primary variable of interest was the difference in RewP amplitude following feedback on lean versus rich trials (ΔRewP), which captures the degree to which the ACC tracks reward probability across different contexts.

fMRI-Based Learning Task: Quantifying Striatal RPEs

Striatal RPE signals were assessed using a well-validated explicit reinforcement learning paradigm (19,56) that required participants to learn reward contingencies through trial and error. On each trial, participants were asked to choose between 2 symbols, where each symbol in the pair was associated with an 80%/20% probability of a given outcome (gain: \$1/\$0; loss: \$0/−\$1; neutral: gray square/nothing). We used Q-learning to calculate the RPE (19) from participants' behavioral data and then imaging analyses focused on a parametric modulation contrast for RPE signals (Supplemental Methods).

Anatomically defined regions of interest in the left and right nucleus accumbens (NAc) were selected from prior research showing links between dopamine transporter function and reward learning (14) (Figure 1C). Beta weights from RPE contrasts were extracted from these regions of interest. A one-sample t test confirmed that the RPE in both regions of interest was >0 [left: $t_{106} = 3.07$, $p = .003$; right: $t_{106} = 4.12$, $p < .001$], so beta values were averaged to create a single NAc RPE beta weight that was used for subsequent analyses. A positive RPE beta value signified higher activation for unexpected reward and lower activation for unexpected omission of rewards during gain trials.

MRS: Quantifying mPFC Glutamate

^{1}H-MRS was used to assess mPFC Gln/Glu. A 2 × 2 × 2-cm voxel was placed in the mPFC, midsagittally, anterior to the genu of the corpus collosum (Figure 1D). The voxel was automatically shimmed, with further manual shimming performed as needed. A modified J-resolved protocol (57) was used to resolve glutamatergic metabolites. This sequence involved the collection of 22 echo time (TE)-stepped spectra with a TE ranging from 35 to 250 ms in 15-ms increments (repetition time = 2 s, f1 acquisition bandwidth = 67 Hz, spectral bandwidth = 2 kHz, readout duration = 512 ms, number of excitations = 16/TE step, approximate scan duration = 12 min).

To quantify glutamate and glutamine with the modified J-resolved protocol data, the 22 TE-stepped free induction decay series was zero filled out to 64 points, Gaussian filtered, and Fourier transformed using gamma-simulated J-resolved basis sets modeled for 2.89T. Every J-resolved spectral extraction within a bandwidth of 67 Hz was fit with the spectral-fitting package LCModel (http://s-provencher.com/pages/lcmodel.shtml) and its theoretically correct template. The integrated area under the entire 2D surface for each metabolite was calculated by summing the raw peak areas across all 64 J-resolved extractions (Supplemental Methods). Our primary outcome was the Gln/Glu ratio.

Statistical Analysis

Multivariable regression analyses examined whether ΔRewP, NAc RPE, or mPFC Gln/Glu predicted anhedonia, (hypo)mania, or impulsivity in the clinical sample cross-sectionally and longitudinally. Separate regression models were run for each outcome (MASQ-AD, BISS-mania, and BIS). Models included covariates (age, sex, and medication load), mood polarity/diagnosis (group: dummy coded with 0 = unipolar and 1 = bipolar), the three neural predictors (ΔRewP, NAc RPE, and mPFC Gln/Glu), and a group × predictor interaction term for each neural predictor. Models predicting follow-up symptom severity also controlled for baseline symptom severity.

RESULTS

Sample Characteristics

The sample was 63.4% female ($n = 71$), with a mean age of 28.6 years (SD = 9.1, range = 18–60). Of the patient group, 72.5% ($n = 58$) had unipolar mood pathology (MDD/dysthymia or MDD in partial remission), 27.5% ($n = 22$) had bipolar mood pathology (BD type I or II, depressed, mixed, or hypomanic), and 40% ($n = 32$) took medication (see Table 1 and Supplemental Methods for details). Sample sizes for each of the analyses varied when a participant had missing data on one or more of the neural indices and/or follow-up measures. Accordingly, sample sizes ranged from 25 to 32 for the control group, from 38 to 58 for the unipolar group, and from 12 to 22 for the bipolar group (sample sizes for the various analyses are specified below).

Table 1. Demographic and Clinical Characteristics of Sample

	HC (n = 32)	Unipolar (n = 58)	Bipolar (n = 22)	Test	p
Demographic Characteristics					
Age, years, mean (±SD)	28.4 (±7.7)	28.0 (±8.6)	30.5 (±12.1)	F = 0.59	.56
Female, n (%)	17 (53.1)	41 (71.7)	13 (59.1)	χ^2 = 2.96	.23
Education, years, mean (±SD)	17.0 (±3.2)	16.0 (±2.8)	15.6 (±3.1)	F = 1.77	.18
White, n (%)	21 (65.6)	40 (69.0)	19 (86.4)	χ^2 = 10.02	.26
Hispanic, n (%)	2 (6.3)	6 (10.3)	2 (9.1)	χ^2 = 0.43	.81
Clinical Diagnoses, n (%)					
Current MDD	–	49 (84.5)	–	–	–
Current dysthymia	–	1 (1.7)	–	–	–
MDD in partial remission	–	8 (13.8)	–	–	–
BD-I depressed	–	–	7 (31.8)	–	–
BD-I mixed	–	–	0 (0.0)	–	–
BD-I hypomanic	–	–	2 (9.1)	–	–
BD-II depressed	–	–	9 (40.9)	–	–
BD-II mixed	–	–	1 (4.6)	–	–
BD-II hypomanic	–	–	3 (13.6)	–	–
Comorbidities, n (%)					
Alcohol abuse	–	0 (0.0)	2 (9.1)	χ^2 = 5.41	.02
EDNOS or BED	–	2 (3.4)	2 (9.1)	χ^2 = 1.07	.30
GAD	–	3 (5.2)	2 (9.1)	χ^2 = 0.42	.52
Panic disorder	–	1 (1.7)	0 (0.0)	χ^2 = 0.38	.54
PTSD	–	3 (5.2)	2 (9.1)	χ^2 = 0.42	.52
Social phobia	–	8 (13.8)	3 (13.6)	χ^2 = 0.00	.99
Specific phobia	–	3 (5.2)	2 (9.1)	χ^2 = 0.42	.52
Medication, n (%)					
Antidepressants	–	19 (32.8)	4 (18.2)	χ^2 = 1.65	.20
Mood stabilizer or anticonvulsant	–	1 (1.7)	7 (31.8)	χ^2 = 16.05	<.001
Anticonvulsants	–	0 (0.0)	1 (4.5)	χ^2 = 2.67	.10

All tests are two tailed.

BD-I/II, bipolar disorder type I/II; BED, binge eating disorder; EDNOS, eating disorder not otherwise specified; GAD, generalized anxiety disorder; HC, healthy control group; MDD, major depressive disorder; PTSD, posttraumatic-traumatic stress disorder.

Correlations Among Units

Pearson correlations were used to determine the degree to which the three neural indices mapped onto behavioral reward learning (see Tables S1 and S2; differences in units of analysis between diagnostic groups are reported in the Supplemental Results and Figure S2). Across the sample, higher mPFC Gln/Glu correlated with better reward learning (r = .27, p = .007; n = 102) (Figure S3A). This was consistent with the linear trend shown in Figure S3A, where mPFC Gln/Glu values increased across the learning quintiles. Furthermore, the quintiles explained a greater proportion of the variance in mPFC Gln/Glu relative to diagnosis (5% vs. 2%; R^2 change = .05, F change = 5.25, p = .02).

Although ΔRewP and NAc RPE were not correlated with our a priori–defined learning measure (block 3 minus block 1 response bias), they were correlated with the total overall response bias. Specifically, heightened NAc RPE (r = .37, p = .04; n = 32) (Figure S3B) and ΔRewP (r = .41, p = .04; n = 25) (Figure S3C) correlated with greater overall response bias in control subjects but not in patients (p > .10, n = 75). Furthermore, across the whole sample, heightened NAc RPE was associated with faster learning in block 1 (r = .23, p = .02; n = 107).

Elevated mPFC Gln/Glu Correlates With More Severe (Hypo)manic Symptoms Cross-Sectionally

Standardized values for each outcome measure across the reward learning quintiles are shown in Figure S4 (patients only). Multimodal regression models assessed whether the three reward circuit markers were associated with symptom severity cross-sectionally.

A significant group × mPFC Gln/Glu interaction (β = .28, p = .04; n = 57) emerged from the model predicting baseline (hypo)mania severity (BISS-mania), indicating that the effect of mPFC Gln/Glu on baseline (hypo)mania severity differed across the unipolar and bipolar groups (Table 2). To unpack this interaction, we examined the correlation between mPFC Gln/Glu and baseline BISS-mania scores (both residualized for other variables in the model) in each group. mPFC Gln/Glu was associated with higher BISS-mania scores in the bipolar group (r = .56, p = .045; n = 13) but not in the unipolar group (r = −.24, p = .12; n = 45).

In contrast, none of the neural indices predicted anhedonia severity (MASQ-AD) or impulsivity (BIS) (all ps > .05) cross-sectionally.

Table 2. Models Predicting (Hypo)manic Symptom Severity on the BISS-mania Scale

	B	SE	β	*t*	*p*
Dependent Variable: Baseline (Hypo)manic Symptom Severity					
(Constant)	9.14	2.33		3.92	<.001
Age	−0.09	0.08	−.13	−1.18	.24
Sex	−2.77	1.52	−.20	−1.82	.08
Medication load	−0.71	0.42	−.19	−1.71	.09
Group	10.46	1.60	.69	6.52	<.001
ΔRewP	−0.70	1.24	−.07	−0.56	.58
NAc RPE	0.03	0.57	.01	0.05	.96
mPFC Gln/Glu	−9.33	16.39	−.07	−0.57	.57
Group × ΔRewP	−1.48	2.27	−.09	−0.65	.52
Group × NAc RPE	2.11	1.90	.13	1.11	.27
Group × mPFC Gln/Glu	68.06	31.51	.28	2.16	.04
Dependent Variable: 3-Month (Hypo)manic Symptom Severity					
(Constant)	3.49	1.93		1.81	.08
Age	0.06	0.06	.15	0.99	.33
Sex	−2.14	1.19	−.27	−1.80	.08
Medication load	−0.29	0.32	−.12	−0.90	.37
Baseline BISS-mania	0.16	0.11	.28	1.54	.13
Group	−1.15	1.61	−.13	−0.71	.48
ΔRewP	−1.02	0.99	−.16	−1.03	.31
NAc RPE	−0.04	0.43	−.01	−0.10	.92
mPFC Gln/Glu	−38.43	14.30	−.46	−2.69	.01
Group × ΔRewP	1.03	1.93	.08	0.53	.60
Group × NAc RPE	−0.07	1.35	−.01	−0.05	.96
Group × mPFC Gln/Glu	96.92	24.90	.70	3.89	<.001

Group was dummy coded (0 = unipolar, 1 = bipolar).

BISS-mania, Mania subscale score of Bipolar Inventory of Symptoms Scale; RewP, reward positivity; NAc RPE, nucleus accumbens reward prediction error; mPFC Gln/Glu, medial prefrontal cortex ratio of glutamine to glutamate.

Elevated mPFC Gln/Glu Correlates With More Severe (Hypo)manic Symptoms Longitudinally

Next, we examined whether, after controlling for baseline (hypo)manic severity, the reward circuit markers were associated with 3- and 6-month follow-up symptom severity (see Figure S5 for mean symptom severity across time). A group × mPFC Gln/Glu interaction (β = .70, $p < .001$; $n = 49$) emerged for the model predicting 3-month BISS-mania scores (Table 2). To unpack this interaction, we again examined the correlation between mPFC Gln/Glu and 3-month BISS-mania scores (residualized for other variables in the model) in each group. Increased mPFC Gln/Glu was associated with less severe hypomanic symptoms in the unipolar group ($r = -.35$, $p = .03$; $n = 38$) but with more severe hypomanic symptoms in the bipolar group ($r = .85$, $p < .001$; $n = 12$) (Figure 3) at 3 months.

In contrast, the reward learning markers did not predict 6-month follow-up BISS-mania scores or 3- or 6-month MASQ-AD or BIS scores (all $ps > .05$) (see Supplemental Results for exploratory unimodal analyses).

Predictive Value of mPFC Gln/Glu

Next, we compared a simple model containing covariates (age, sex, medication load, and baseline BISS-mania) and diagnostic information (group) with a model containing terms for mPFC Gln/Glu and group × mPFC Gln/Glu. The simple model explained 15.8% of the variance in 3-month (hypo)manic symptom severity, $F_{5,44} = 1.65$, $p = .17$. However, adding the mPFC Gln/Glu terms explained an additional 24.3% of the variance in 3-month hypomanic symptom severity, $F_{7,42} = 4.01$, $p = .002$, and this change in R^2 was significant (F change = 8.49, R^2 change = .24, $p = .001$). This indicates that mPFC Gln/Glu explained greater variance in future hypomanic symptom severity relative to baseline diagnosis alone. Furthermore, we confirmed that mPFC Gln/Glu explained a greater proportion of the variance in 3-month (hypo)manic symptom severity relative to behavioral reward learning alone (F change = 3.91, R^2 change = .09, $p = .03$) (Table S3), indicating that adding this biomarker enhanced predictive power over and above behavioral data.

DISCUSSION

Using a novel recruitment method, a transdiagnostic sample, and a multimodal longitudinal design, we examined whether variation along the RDoC Positive Valence Systems domain of reward learning and the underlying neurocircuitry predicted variability in three reward-related mood symptoms: anhedonia, (hypo)mania, and impulsivity. In doing so, we focused on three components of reward learning neurocircuitry linked to mood disorder pathophysiology that span distinct units of analysis across physiology (ACC-mediated PEs), circuits (striatal RPEs), and molecules (mPFC Gln/Glu).

As predicted, the three neural components correlated with aspects of behavioral reward learning on the PRT. In terms of symptoms, elevated mPFC Gln/Glu predicted more severe cross-sectional and longitudinal (hypo)manic symptoms in those with bipolar pathology. Importantly, baseline mPFC Gln/Glu levels explained a greater proportion of the variance in (hypo)manic symptoms at 3 months relative to diagnosis alone. These findings extend prior case-control MRS studies (41,42) by showing that elevated mPFC Gln/Glu is also associated with (hypo)mania severity dimensionally.

We replicated prior findings linking blunted ΔRewP amplitude with greater anhedonia in exploratory unimodal analyses (see Supplement); however, neither ΔRewP nor NAc RPE signals were associated with symptom severity when entered into a multimodal model with mPFC Gln/Glu. Although the lack of a relationship between NAc RPE and anhedonia in our unimodal analyses contrasts with recent findings showing that striatal RPEs predicted improvement in anhedonic symptoms (58), we used a more complex instrumental fMRI learning paradigm designed to assess striatal RPEs in the context of learning as opposed to a more traditional guessing-type paradigm (which maximizes the RPE signal yet involves minimal learning).

It is important to consider what these findings mean for an RDoC approach to mood disorder classification that remains agnostic to DSM diagnoses. On the one hand, mPFC Gln/Glu correlated with reward learning across diagnoses, providing converging evidence that mPFC Gln/Glu is a transdiagnostic marker of this RDoC domain. In addition, in a heterogeneous

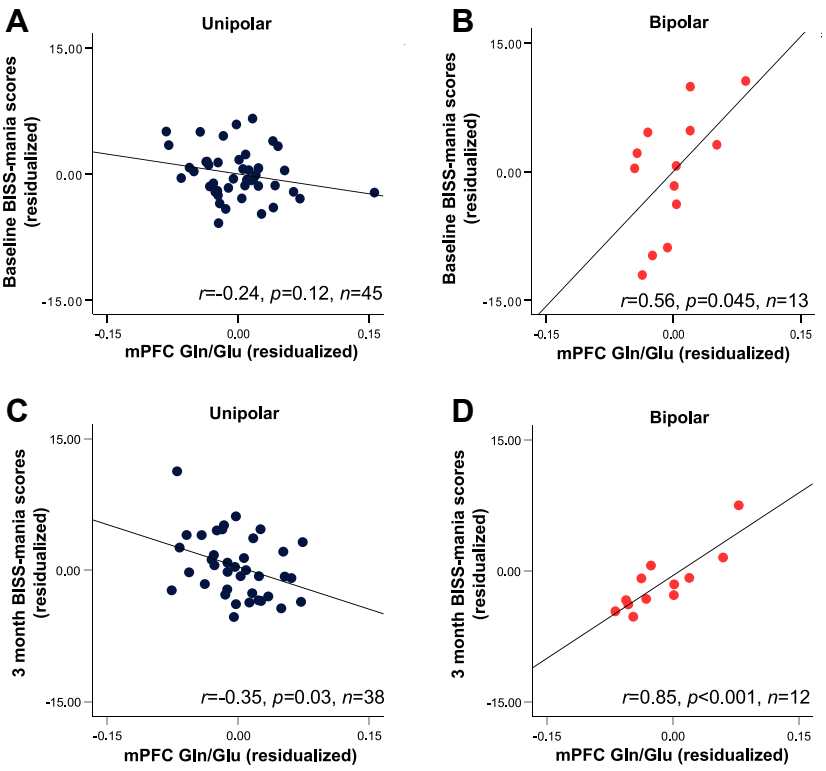

Figure 3. Group × medial prefrontal cortex (mPFC) glutamine/glutamate (Gln/Glu) interaction for longitudinal (hypo)manic symptom severity. Residualized scatter plots show the relationship between mPFC Gln/Glu and (hypo)manic symptom severity (Mania subscale scores of the Bipolar Inventory of Symptoms Scale [BISS-mania]) at baseline **(A, B)** and at the 3-month follow-up assessment **(C, D)** in the unipolar and bipolar mood disorder groups. Residualized values on each axis control for the other variables in the model, which were age, sex, baseline BISS-mania subscale scores, change in reward positivity amplitude, and nucleus accumbens reward prediction error beta weights.

sample, more homogeneity in neurobiology (mPFC Gln/Glu levels) was observed within groups when groups were defined on the basis of reward learning versus diagnostic categories. This is consistent with the RDoC's assumption that dimensions of functioning are more proximal to neurobiology than to diagnostic categories. Furthermore, dimensional increases in this reward learning biomarker (i.e., mPFC Gln/Glu levels) predicted dimensional increases in symptoms characterized by excessive reward responsiveness (i.e., hypomania) rather than membership in a specific diagnostic category. This echoes one of the RDoC's central theses that abnormalities in circuits and associated constructs likely underpin specific features of mental illness rather than explain any single disorder in its entirety. Together, these findings partly align with a diagnosis-agnostic approach to mood disorder classification.

However, our results also highlight the considerable value of diagnostic information in predicting symptom trajectories. Specifically, although mPFC Gln/Glu correlated with reward learning transdiagnostically, the link between mPFC Gln/Glu and (hypo)manic symptom severity was disease specific and diagnostic information remained an integral component of the final predictive model. If we assume that these findings could inform novel interventions based on neurobiological underpinnings (a key driver of the RDoC approach), then targeting mPFC Gln/Glu may affect reward learning in a similar manner across disorders but have different effects on symptoms in distinct mood disorder subtypes. The degree to which the RDoC framework predicts purely dimensional variability across disorders versus a blend of transdiagnostic and disorder-specific effects remains an important topic of debate. Our findings indicate that while information about reward circuit function could improve the prediction of risk for reward-related clinical symptoms (an important finding in its own right), it would do so in tandem with, rather than independent of, existing diagnostic frameworks.

This study has several strengths. By examining neurobiological mechanisms of reward learning across multiple units of analysis, we could probe reward learning circuitry with superior spatiotemporal resolution and at both micro and macro scales, which cannot be achieved with a single unit or modality alone. Furthermore, we tested whether these units of analysis enhanced the ability to predict clinical course over and above information already used in routine clinical care (diagnosis and baseline symptom severity). Because mPFC Gln/Glu levels can be obtained using MRS in as little as 6 minutes with good test–retest reliability (intraclass correlation coefficient = .803) (59), mPFC Gln/Glu warrants further investigation as a potential screening method for individuals at suspected risk for BD.

However, some limitations of this study must also be noted. First, mPFC Gln/Glu predicted worse (hypo)manic symptoms specifically in individuals with bipolar mood pathology. Because the instance of (hypo)manic symptoms was lower in the unipolar group at follow-up, this may have restricted the variance in symptoms that could be explained by mPFC Gln/Glu. Second, although our three neural indices were selected based on their established association with reward learning,

only mPFC Gln/Glu was associated with our a priori reward learning measure and the three neural indices were not correlated with one another. Although stronger associations may have been evident in a larger sample, the lack of association could also reflect an issue with the construct validity of these units of analysis. For example, it is possible that similar impairments in reward learning may have distinct etiologies (often referred to as equifinality), particularly when considering individuals with very divergent forms of psychopathology. How equifinality is accounted for remains an important conceptual issue for the RDoC framework. Finally, reductions in sample size for longitudinal analyses (resulting from participant attrition and the need to obtain good quality data across all three neural indices) mean that reduced statistical power is a limitation of our study and may explain several null findings. The replicability of these results must be interpreted in light of concerns around the generalizability and reproducibility of neuroimaging findings obtained using small samples (60). Accordingly, rather than being definitive, we interpret these findings as novel yet preliminary insights that warrant replication in larger samples.

In sum, we showed that a key component of reward learning neurocircuitry—mPFC Gln/Glu—predicted worse (hypo)manic symptoms. This marker enhanced the ability to predict future (hypo)mania risk over and above diagnostic information alone. Using this marker to improve precision in the diagnosis and treatment of mood pathology therefore represents an important avenue for future research, with a focus on larger well-powered samples.

ACKNOWLEDGMENTS AND DISCLOSURES

This project was supported by the National Institute of Mental Health (NIMH) (Grant Nos. R01 MH101521 and R37 MH068376 [to DAP]). AEW received support from the National Health and Medical Research Council (Grant No. GNT1110773).

The content is solely the responsibility of the authors and does not necessarily represent the official views of the National Institutes of Health. The funding organizations had no role in the design and conduct of the study; collection, management, analysis, and interpretation of the data; the preparation, review, or approval of the manuscript; and the decision to submit the manuscript for publication.

AEW, PK, and DAP had full access to all the data in the study and take responsibility for the integrity and accuracy of the data. DAP, MTT, and AEW were responsible for study concept and design. AEW was responsible for drafting the manuscript. AEW, DAP, MTT, PK, DF, FD, MLI, and AVR were responsible for critical revision of the manuscript for important intellectual content. AEW, PK, DF, and GF were responsible for statistical analysis. MLI, AVR, and FD were responsible for administrative, technical, or material support. DAP and AEW were responsible for study supervision.

We acknowledge Thilo Deckersbach, Andrew Nierenberg, and Amy Farabaugh for facilitating recruitment of participants through the Depression Clinic and Research Program and the Bipolar Clinic and Research Program at Massachusetts General Hospital and also acknowledge Daniel Ju Hyung Kim, Emily E. Bernstein, and Margaret E. Gigler for their assistance with patient screening and data collection at these two clinics. We also thank Madeline M. Alexander, Laurie A. Scott, Nancy Hall-Brooks, and David J. Crowley for their important contributions to the screening and clinical assessment of participants recruited through the McLean Hospital Center for Depression, Anxiety and Stress Research. Finally, we recognize the critical contributions of J. Eric Jensen, who passed away while this study was being conducted. Dr. Jensen's expertise was integral to the design and implementation of the MRS protocol used in the current study, and this article is dedicated to him.

The findings from this study were presented in part as posters or invited talks at the 2015 (Toronto, Ontario, Canada) and 2019 (Chicago, Illinois) Social of Biological Psychiatry annual meetings, the 2015 (Miami, Florida) and 2017 (San Francisco, California) Anxiety and Depression Association of America annual meetings, and the 2017 (Boston, Massachusetts) Association for Psychological Science annual meeting.

Over the past 3 years, DAP has received funding from the NIMH, the Brain and Behavior Research Foundation, the Dana Foundation, and Millennium Pharmaceuticals; consulting fees from BlackThorn Therapeutics, Boehringer Ingelheim, Compass Pathway, Concert Pharmaceuticals, Engrail Therapeutics, Neurocrine Biosciences, Otsuka Pharmaceuticals, and Takeda Pharmaceuticals; one honorarium from Alkermes; and stock options from BlackThorn Therapeutics. DAP has a financial interest in BlackThorn Therapeutics, which has licensed the copyright to the PRT through Harvard University. DAP's interests were reviewed and are managed by McLean Hospital and Partners HealthCare in accordance with their conflict of interest policies. All other authors report no biomedical financial interests or potential conflicts of interest.

ClinicalTrials.gov: Brain Mechanisms of Human Motivation; https://clinicaltrials.gov/ct2/show/NCT01976975; NCT01976975.

ARTICLE INFORMATION

From the Center for Depression, Anxiety and Stress Research (AEW, PK, AVR, MLI, GF, FD, DAP), McLean Hospital, Belmont, and Department of Psychiatry (AEW, PK, AVR, MLI, GF, FD, DAP), Harvard Medical School, Boston, Massachusetts; Department of Psychology (MTT), Emory University, Atlanta, Georgia; Department of Psychological Sciences (DF), Purdue University, West Lafayette, Indiana; and Black Dog Institute (AEW), University of New South Wales, Randwick, New South Wales, Australia.

Address correspondence to Diego A. Pizzagalli, Ph.D., at dap@mclean.harvard.edu.

Received Nov 12, 2020; revised Dec 25, 2020; accepted Jan 7, 2021.

Supplementary material cited in this article is available online at https://doi.org/10.1016/j.bpsc.2021.01.004.

REFERENCES

1. American Psychiatric Association (2013): Diagnostic and Statistical Manual of Mental Disorders, 5th ed. Washington, DC: American Psychiatric Publishing.
2. World Health Organization (2018): International Classification of Diseases for Mortality and Morbidity Statistics, 11th revision Geneva, Switzerland: World Health Organization.
3. Yatham LN, Kennedy SH, Parikh SV, Schaffer A, Bond DJ, Frey BN, *et al.* (2018): Canadian Network for Mood and Anxiety Treatments (CANMAT) and International Society for Bipolar Disorders (ISBD) 2018 guidelines for the management of patients with bipolar disorder. Bipolar Disord 20:97–170.
4. Goodwin G, Haddad P, Ferrier I, Aronson J, Barnes T, Cipriani A, *et al.* (2016): Evidence-based guidelines for treating bipolar disorder: Revised third edition recommendations from the British Association for Psychopharmacology. J Psychopharmacol 30:495–553.
5. Cuthbert BN, Insel TR (2013): Toward the future of psychiatric diagnosis: The seven pillars of RDoC. BMC Med 11:126.
6. Cuthbert BN (2014): The RDoC framework: Facilitating transition from ICD/DSM to dimensional approaches that integrate neuroscience and psychopathology. World Psychiatry 13:28–35.
7. Whitton AE, Treadway MT, Pizzagalli DA (2015): Reward processing dysfunction in major depression, bipolar disorder and schizophrenia. Curr Opin Psychiatry 28:7–12.
8. Alloy LB, Nusslock R, Boland EM (2015): The development and course of bipolar spectrum disorders: An integrated reward and circadian rhythm dysregulation model. Annu Rev Clin Psychol 11:213–250.
9. Pizzagalli DA, Goetz E, Ostacher M, Iosifescu DV, Perlis RH (2008): Euthymic patients with bipolar disorder show decreased reward learning in a probabilistic reward task. Biol Psychiatry 64:162–168.

10. Pizzagalli DA, Iosifescu D, Hallett LA, Ratner KG, Fava M (2008): Reduced hedonic capacity in major depressive disorder: Evidence from a probabilistic reward task. J Psychiatric Res 43:76–87.
11. Vrieze E, Pizzagalli DA, Demyttenaere K, Hompes T, Sienaert P, de Boer P, *et al.* (2013): Reduced reward learning predicts outcome in major depressive disorder. Biol Psychiatry 73:639–645.
12. Pizzagalli DA, Evins AE, Schetter EC, Frank MJ, Pajtas PE, Santesso DL, Culhane M (2008): Single dose of a dopamine agonist impairs reinforcement learning in humans: Behavioral evidence from a laboratory-based measure of reward responsiveness. Psychopharmacology 196:221–232.
13. Santesso DL, Evins AE, Frank MJ, Schetter EC, Bogdan R, Pizzagalli DA (2009): Single dose of a dopamine agonist impairs reinforcement learning in humans: Evidence from event-related potentials and computational modeling of striatal-cortical function. Hum Brain Mapp 30:1963–1976.
14. Kaiser RH, Treadway MT, Wooten DW, Kumar P, Goer F, Murray L, *et al.* (2018): Frontostriatal and dopamine markers of individual differences in reinforcement learning: A multi-modal investigation. Cereb Cortex 28:4281–4290.
15. Bogdan R, Pizzagalli DA (2009): The heritability of hedonic capacity and perceived stress: A twin study evaluation of candidate depressive phenotypes. Psychol Med 39:211–218.
16. Schultz W (2015): Neuronal reward and decision signals: From theories to data. Physiol Rev 95:853–951.
17. Balleine BW, O'Doherty JP (2010): Human and rodent homologies in action control: Corticostriatal determinants of goal-directed and habitual action. Neuropsychopharmacology 35:48–69.
18. Daw ND, Niv Y, Dayan P (2005): Uncertainty-based competition between prefrontal and dorsolateral striatal systems for behavioral control. Nat Neurosci 8:1704–1711.
19. Pessiglione M, Seymour B, Flandin G, Dolan RJ, Frith CD (2006): Dopamine-dependent prediction errors underpin reward-seeking behaviour in humans. Nature 442:1042–1045.
20. Schultz W, Dayan P, Montague PR (1997): A neural substrate of prediction and reward. Science 275:1593–1599.
21. Gläscher J, Daw N, Dayan P, O'Doherty JP (2010): States versus rewards: Dissociable neural prediction error signals underlying model-based and model-free reinforcement learning. Neuron 66:585–595.
22. Schultz W (2016): Dopamine reward prediction-error signalling: A two-component response. Nat Rev Neurosci 17:183–195.
23. Kumar P, Goer F, Murray L, Dillon DG, Beltzer ML, Cohen AL, *et al.* (2018): Impaired reward prediction error encoding and striatal-midbrain connectivity in depression. Neuropsychopharmacology 43:1581–1588.
24. Whitton AE, Reinen JM, Slifstein M, Ang Y-S, McGrath PJ, Iosifescu DV, *et al.* (2020): Baseline reward processing and ventrostriatal dopamine function are associated with pramipexole response in depression. Brain 143:701–710.
25. Kumar P, Waiter G, Ahearn T, Milders M, Reid I, Steele J (2008): Abnormal temporal difference reward-learning signals in major depression. Brain 131:2084–2093.
26. Nusslock R, Almeida JR, Forbes EE, Versace A, Frank E, LaBarbara EJ, *et al.* (2012): Waiting to win: Elevated striatal and orbitofrontal cortical activity during reward anticipation in euthymic bipolar disorder adults. Bipolar Disord 14:249–260.
27. O'Sullivan N, Szczepanowski R, El-Deredy W, Mason L, Bentall RP (2011): fMRI evidence of a relationship between hypomania and both increased goal-sensitivity and positive outcome-expectancy bias. Neuropsychologia 49:2825–2835.
28. Abler B, Greenhouse I, Ongur D, Walter H, Heckers S (2008): Abnormal reward system activation in mania. Neuropsychopharmacology 33:2217–2227.
29. Proudfit GH (2015): The reward positivity: From basic research on reward to a biomarker for depression. Psychophysiology 52:449–459.
30. Foti D, Weinberg A, Dien J, Hajcak G (2011): Event-related potential activity in the basal ganglia differentiates rewards from nonrewards: Response to commentary. Hum Brain Mapp 32:2267–2269.
31. Santesso DL, Dillon DG, Birk JL, Holmes AJ, Goetz E, Bogdan R, Pizzagalli DA (2008): Individual differences in reinforcement learning: Behavioral, electrophysiological, and neuroimaging correlates. NeuroImage 42:807–816.
32. Whitton AE, Kakani P, Foti D, Van't Veer A, Haile A, Crowley DJ, Pizzagalli DA (2016): Blunted neural responses to reward in remitted major depression: A high-density event-related potential study. Biol Psychiatry Cogn Neurosci Neuroimaging 1:87–95.
33. Mason L, O'Sullivan N, Blackburn M, Bentall R, El-Deredy W (2012): I want it now! Neural correlates of hypersensitivity to immediate reward in hypomania. Biol Psychiatry 71:530–537.
34. Foti D, Hajcak G (2009): Depression and reduced sensitivity to non-rewards versus rewards: Evidence from event-related potentials. Biol Psychol 81:1–8.
35. Bress JN, Foti D, Kotov R, Klein DN, Hajcak G (2013): Blunted neural response to rewards prospectively predicts depression in adolescent girls. Psychophysiology 50:74–81.
36. Holroyd CB, Coles MG (2002): The neural basis of human error processing: Reinforcement learning, dopamine, and the error-related negativity. Psychol Rev 109:679–709.
37. Geisler S, Derst C, Veh RW, Zahm DS (2007): Glutamatergic afferents of the ventral tegmental area in the rat. J Neurosci 27:5730–5743.
38. Hauber W, Sommer S (2009): Prefrontostriatal circuitry regulates effort-related decision making. Cereb Cortex 19:2240–2247.
39. Jocham G, Hunt LT, Near J, Behrens TE (2012): A mechanism for value-guided choice based on the excitation-inhibition balance in prefrontal cortex. Nat Neurosci 15:960–961.
40. Pellerin L, Magistretti PJ (2004): Let there be (NADH) light. Science 305:50–52.
41. Yüksel C, Öngür D (2010): Magnetic resonance spectroscopy studies of glutamate-related abnormalities in mood disorders. Biol Psychiatry 68:785–794.
42. Gigante AD, Bond DJ, Lafer B, Lam RW, Young LT, Yatham LN (2012): Brain glutamate levels measured by magnetic resonance spectroscopy in patients with bipolar disorder: A meta-analysis. Bipolar Disord 14:478–487.
43. Öngür D, Jensen JE, Prescot AP, Stork C, Lundy M, Cohen BM, Renshaw PF (2008): Abnormal glutamatergic neurotransmission and neuronal-glial interactions in acute mania. Biol Psychiatry 64:718–726.
44. Frye MA, Watzl J, Banakar S, O'Neill J, Mintz J, Davanzo P, *et al.* (2007): Increased anterior cingulate/medial prefrontal cortical glutamate and creatine in bipolar depression. Neuropsychopharmacology 32:2490–2499.
45. Kubo H, Nakataki M, Sumitani S, Iga J-I, Numata S, Kameoka N, *et al.* (2017): ^{1}H-magnetic resonance spectroscopy study of glutamate-related abnormality in bipolar disorder. J Affect Disord 208:139–144.
46. Pizzagalli DA, Jahn AL, O'Shea JP (2005): Toward an objective characterization of an anhedonic phenotype: A signal-detection approach. Biol Psychiatry 57:319–327.
47. First MB, Spitzer RL, Gibbon M, Williams JB (2002): Structured Clinical Interview for DSM-IV-TR Axis I Disorders, Research Version, Patient Edition (SCID-I/P). New York: New York State Psychiatric Institute.
48. Young RC, Biggs JT, Ziegler VE, Meyer DA (1978): A rating scale for mania: Reliability, validity and sensitivity. Br J Psychiatry 133:429–435.
49. Watson D, Weber K, Assenheimer JS, Clark LA, Strauss ME, McCormick RA (1995): Testing a tripartite model: I. Evaluating the convergent and discriminant validity of anxiety and depression symptom scales. J Abnorm Psychol 104:3–14.
50. Patton JH, Stanford MS, Barratt ES (1995): Factor structure of the Barratt Impulsiveness Scale. J Clin Psychol 51:768–774.
51. Gonzalez JM, Bowden CL, Katz MM, Thompson P, Singh V, Prihoda TJ, Dahl M (2008): Development of the Bipolar Inventory of Symptoms Scale: Concurrent validity, discriminant validity and retest reliability. Int J Methods Psychiatr Res 17:198–209.
52. Macmillan N, Creelman C (1991): Detection Theory: A User's Guide. Cambridge, UK: Cambridge University Press.
53. Hautus MJ (1995): Corrections for extreme proportions and their biasing effects on estimated values of d'. Behav Res Methods Instrum Comput 27:46–51.

54. Dien J (2010): The ERP PCA Toolkit: An open source program for advanced statistical analysis of event-related potential data. J Neurosci Methods 187:138–145.
55. Pascual-Marqui RD (2002): Standardized low-resolution brain electromagnetic tomography (sLORETA): Technical details. Methods Find Exp Clin Pharmacol 24:5–12.
56. Treadway MT, Admon R, Arulpragasam AR, Mehta M, Douglas S, Vitaliano G, *et al.* (2017): Association between interleukin-6 and striatal prediction-error signals following acute stress in healthy female participants. Biol Psychiatry 82:570–577.
57. Brennan BP, Tkachenko O, Schwab ZJ, Juelich RJ, Ryan EM, Athey AJ, *et al.* (2015): An examination of rostral anterior cingulate cortex function and neurochemistry in obsessive–compulsive disorder. Neuropsychopharmacology 40:1866–1876.
58. Eckstrand KL, Forbes EE, Bertocci MA, Chase HW, Greenberg T, Lockovich J, *et al.* (2019): Anhedonia reduction and the association between left ventral striatal reward response and 6-month improvement in life satisfaction among young adults. JAMA Psychiatry 8:958–965.
59. Jensen JE, Auerbach RP, Pisoni A, Pizzagalli DA (2017): Localized MRS reliability of in vivo glutamate at 3 T in shortened scan times: A feasibility study. NMR Biomed 30:e3771.
60. Sui J, Jiang R, Bustillo J, Calhoun VJBP (2020): Neuroimaging-based individualized prediction of cognition and behavior for mental disorders and health: Methods and promises. Biol Psychiatry 88:818–828.

Mapping Disease Course Across the Mood Disorder Spectrum Through a Research Domain Criteria Framework

Supplementary Information

Supplementary Methods

Inclusion/exclusion criteria

Participants seeking treatment for mood pathology were recruited from the Depression Clinical and Research Center and the Bipolar Clinical and Research Center at Massachusetts General Hospital, as well as from the Center for Depression, Anxiety and Stress Research at McLean Hospital. Healthy controls were recruited from the community.

General inclusion criteria for all participants:

1) Ability to provide written, informed consent
2) Right-handed
3) Normal or corrected-to-normal vision and hearing
4) Fluency in written and spoken English

General exclusion criteria for all participants:

1) Left-handed or ambidextrous
2) Current drug use (cocaine, cannabis, opiates, amphetamines, benzodiazepines, barbiturates), as indicated by a positive urine drug screen on the day of testing
3) Current use of medications with potent dopaminergic effects, including stimulants or antipsychotics, or any use of antidopaminergic medications in the past 6 months
4) Recent use of any medication that affects blood flow or pressure
5) Current use of antibiotics
6) Pregnant women (as indicated by urine pregnancy test on the day of the MRI scan)
7) Serious unstable medical illness
8) Self-reported hypothyroidism
9) History or current diagnosis of dementia
10) History of chronic migraine (>15 days/month) or seizure disorder
11) A history of significant head injury or loss of consciousness for 2 minutes or longer

12) MRI contraindications
13) A score of < 25 on the Mini Mental State Exam at screening

Inclusion criteria specific to the healthy control group:

1) Absence of any past or current use of psychotropic medication
2) Absence of any past or current DSM-IV psychiatric disorders
3) Absence of first-degree relatives with a mood or psychotic disorder
4) No Beck Depression Inventory-II score greater than 9

Exclusion criteria specific to the healthy control group:

1) Use of any other drug or herbal supplement with well-characterized psychotropic effects (e.g., prednisone or St. John's Wort) within the past three weeks
2) Use of any medications within the past 24 hours (e.g., antihistamines, pain relivers, or over-the-counter medication)

Inclusion criteria specific to the mood pathology group:

1) Non-psychotic individual seeking treatment for mood-related symptoms at the Massachusetts General Hospital (MGH) Depression Clinical and Research Program, MGH Bipolar Clinical and Research Program or McLean Hospital
2) Depressive or hypomanic symptoms severe enough to cause distress or impairment, and warrant intervention
3) The depressive or hypomanic symptoms are not secondary to another Axis-I DSM-IV psychiatric disorder, or due to the effects of a substance
4) Stable antidepressant or mood stabilizing medication over the past 8 weeks, or an absence of any psychotropic medication for at least two weeks

Exclusion criteria specific to the mood pathology group:

1) A current diagnosis of obsessive compulsive disorder (OCD), bulimia, alcohol dependence, substance abuse or substance dependence
2) A history or current diagnosis of a psychotic disorder, stimulant dependence or anorexia
3) Suicidal ideation where outpatient treatment is determined unsafe by the study clinical interviewer
4) Electroconvulsive therapy within the past two years

Screening procedures

Consent and initial screening

The flow of participants into the study is shown in Figure S1. After providing written informed consent, all participants answered a series of screening questions about their medical history, current medication and drug use, and the presence of any MR contraindications. Next, participants performed a urine drug screen, after which the experimenter administered the Mini Mental State Exam (1). Participants deemed eligible to continue were then asked to complete the Probabilistic Reward Task (PRT) (2). Participants were permitted to seek treatment while enrolled in the study, as long as the treatment was not listed on the exclusion criteria. Participants received $15/hr in compensation plus earnings on the behavioral and imaging tasks.

Initial assessment of reward learning

Following completion of the PRT, data were immediately scored and quality control checking was performed (as described previously; 2) while the participant waited. Trials with reaction time faster (RT) than 150 ms or slower than 2500 ms were excluded, as were trials where the RT fell outside of ± 3SD from the mean (after applying a logarithmic transformation). Participants were excluded if more than 20 trials in any block were invalid (up to 10 of these trials could be reaction time outliers). Additionally, participants were required to perform at above chance accuracy (≥55%) to ensure that they were exposed to the intended asymmetrical (3:1) reinforcement schedule (the minimum ratio of rich to lean rewards accepted was 2.5:1). If their data passed quality control, healthy controls then underwent clinical assessment using the SCID-IV (3). For individuals with mood pathology who had valid PRT data, their performance was compared to an existing normative distribution in order to determine who would be invited to proceed with the rest of the study (see below).

Matching of reward learning to normative sample

For the mood pathology participants, following quality control checking, the reward learning metric (i.e., response bias in block 3 minus block 1) was computed and compared to an existing normative database of PRT performance in healthy controls (N=572). Recruitment occurred such that we aimed to test an equal number of individuals in each quintile of reward learning performance (i.e., n=16), according to this normative distribution. Participants were excluded from participating further if the quintile in which their reward learning performance fell

was already full. If their reward learning performance fell in a non-full quintile, participants then proceeded to the clinical assessment.

Testing sites

Participants completed five study visits: 1 screening session, 2 imaging visits, and 2 follow-up visits at 3 and 6 months. The first visit was conducted at the Center for Depression, Anxiety and Stress Research at McLean Hospital, the Depression Clinical and Research Program and Massachusetts General Hospital, or the Bipolar Clinical and Research Program at Massachusetts General Hospital. The remaining visits were conducted at McLean Hospital.

Baseline clinical assessments

Participants underwent clinical assessment with the Structured Clinical Interview for DSM-IV to assess for the presence of lifetime Axis I psychiatric disorders (3). The interview was carried out by Masters- or PhD-level trained clinical interviewers. A series of clinician-administered and self-report scales were also administered at baseline to assess clinical symptoms. Anhedonia severity was assessed using the Anhedonic Depression subscale of the Mood and Anxiety Symptom Questionnaire (MASQ-AD) (4). Initial screening for the presence of depressive symptoms was conducted using the Beck Depression Inventory-II (5). This was primarily used to determine eligibility for the healthy control group, who were required to score 9 or lower in order to take part in the study. In addition, (hypo)manic symptoms were screened using the clinician-administered Young Mania Rating Scale (YMRS) (6). For individuals who were invited to take part in the neuroimaging sessions, a more comprehensive assessment of (hypo)manic symptom severity was also performed using the clinician-administered mania subscale of the Bipolar Inventory of Symptoms Scale (BISS-mania) (7). Self-reported impulsivity was also measured using the Barratt Impulsiveness Scale (BIS) (8). In the current study, the MASQ-AD subscale, BISS-mania subscale, and BIS had good internal consistency (Cronbach's alpha values at baseline: MASQ-AD=0.98; BISS-mania=0.85; BIS=0.88).

Quantifying psychotropic medication load

Medication type, dosage and duration of use were obtained at the baseline clinical assessment. Using this information, medication load was calculated using a previously established

method (9) that quantifies the potency of antidepressant medications, as well as the equivalent potency of other psychotropic medications (e.g., mood stabilizers, anticonvulsants, benzodiazepines) and non-pharmacological antidepressant interventions (e.g., electroconvulsive therapy, phototherapy, herbal supplements). This method yielded a single continuous score for each participant that reflected the antidepressant potency of the medication (and other potential interventions) they were taking at the time of assessment.

Follow-up clinical assessments

Participants completed the MASQ-AD, BISS-mania and BIS again at 3- and 6-month follow-up sessions to track changes in clinical symptoms. In addition, diagnosis was re-confirmed using the Longitudinal Interval Follow-up Evaluation (10), and any changes in medication or treatment were recorded.

EEG acquisition and preprocessing

Scalp EEG was recorded using a 128-channel Hydrocel Geodesic Sensor Net system (Electrical Geodesics, Inc.) and sampled at 250Hz (bandwidth, 0.1-100Hz; impedances < 100kΩ). Signals were referenced to the vertex (Cz) at acquisition. Data were preprocessed offline using BrainVision Analyzer 2.0 (Brain Products GmbH). First, horizontal eye movements, vertical eye movements and electrocardiographic artifacts were removed using independent components analysis (11) and noisy channels were interpolated using a spherical spline interpolation (12). Second, data were re-referenced to the average reference, filtered (0.1-30Hz) and epochs extracted from –500ms to 1000ms around presentation of reward feedback on correct rich and correct lean trials. Third, each epoch was visually inspected, and remaining artifacts were removed. Artifacts were rejected using a semi-automated procedure with a maximal allowed voltage step of 50μV between sample points, a maximal voltage difference of 150μV within a 100ms interval, and a minimum allowed voltage of 0.5μV within a 100ms interval. Fourth, epochs were baseline-corrected (-250ms to -50ms) and averaged.

Temporo-spatial principal components analysis of ERP data

A temporo-spatial principal components analysis was used to decompose the time-domain ERP. Temporal variance in the averaged ERP waveforms was examined using temporal PCA and

Infomax rotation. Based on the resulting scree plot, 12 temporal factors were retained for rotation. The spatial distribution of these temporal factors was then examined using spatial PCA and Infomax rotation, with a spatial PCA being conducted for each temporal factor. Eight spatial factors were retained for each temporal factor. Analyses focused on the PCA component most representative of the RewP (TF8/SF2).

Confirmation of ACC source generator for the RewP

Standardized low-resolution electromagnetic tomography (sLORETA) (13) was used to identify the neural generators of the RewP. To do this, we extracted the peak amplitude of the RewP PCA component on rich trials (the peak occurred from 248-252ms post-feedback) and used sLORETA to regress this value on mean current source density across the whole brain from -20ms to +20ms around this peak on rich trials. This analysis revealed voxels where variation in RewP amplitude correlated with variations in current source density. Images were thresholded at $p<0.005$ uncorrected. As shown in Figure 1A in the main text, results revealed a cluster in Brodmann area 32 (corresponding to the dorsal ACC), where current source density was correlated with RewP amplitude. These findings are therefore consistent with our hypothesis that the RewP reflects an ACC-mediated prediction error signal.

fMRI-based instrumental reinforcement learning task

To assess RPE signals, participants completed a well-validated reinforcement learning paradigm (14) during fMRI scanning. On each trial, participants were instructed to choose between two symbols (letters from the Agathodaimon font) displayed on a screen. On every run there were three symbol pairs that were each associated with an 80%/20% probability of a given outcome: Gain ($5/Nothing), Loss (Nothing/-$5), Neutral ($0/Nothing). For each trial, one symbol pair was randomly presented, with one symbol being displayed above and one below a central fixation cross (counterbalanced). Participants were instructed to choose the upper symbol by pressing a key, or to refrain from responding in order to choose the bottom symbol. After a jittered delay interval, participants received outcome feedback: “Gain”, “Loss”, “Nothing” or a grey square with no monetary value for neutral trials. To win money, participants had to learn, by trial and error, the stimulus-outcome contingency. There were three runs across the experiment each lasting approximately 10.5 minutes, consisting of 72 trials (24 per condition), and containing new pairs

of symbols. Participants were told that one of the runs would be randomly selected for the total winnings (in reality, all participants were given the same fixed amount of $40).

Computational model (Q-learning)

A standard Q-learning algorithm was used to calculate the prediction error based on participant's choice and feedback history (15). For each trial, the model estimated the expected value of A (Q_A) and B (Q_B), each of which corresponded to the reward that was expected to be obtained by choosing a particular cue. Q values were set to zero at the beginning of each run. After every trial, $Q_A(t)$ or $Q_B(t)$ were updated based on the feedback participants received in that trial, R(t), per the following rule:

$$Q_{chosen\_cue}(t+1) = Q_{chosen\_cue}(t) + \alpha\, \delta(t),$$

where α is the learning rate parameter and δ is the prediction error.

The prediction error is defined as the difference between the expected reward [$Q_{chosen\_cue}(t)$] and the actual reward received [R(t)], i.e.:

$$\delta(t) = R(t) = Q_{chosen\_cue}(t),$$

where R is assigned a value of 1 for reward and 0 for no reward during gain trials, and a value of 0 for no punishment and -1 for punishment during loss trials.

Based on the Q values on any given trial, the probability of choosing a particular symbol was calculated using the softmax rule, such that the probability of choosing symbol A was:

$$P_A(t) = \exp(Q_A(t)/\beta)/[\exp(Q_A(t)/\beta) + \exp(Q_B(t)/\beta)]$$

We chose a fixed learning rate of alpha=0.4 and beta=0.1 because this most closely approximated the average alpha (M±SD=0.39±0.17) and beta (0.14±0.17) across all subjects and runs of the task.

fMRI acquisition

Data were acquired at the McLean Imaging Center using a 3-Tesla Siemens Tim Trio scanner with a 32-channel head coil. Trial presentation was synchronized to the initial volume acquisition. Functional MRI data were acquired using a gradient echo T2*-weighted echo planar imaging sequence with 30 degree titled slice acquisition to mitigate signal loss in regions affected by susceptibility artifacts, with the following acquisition parameters: repetition time (TR) = 3000ms; echo time (TE) = 30ms; field of view (FOV) = 224mm; voxel dimensions = 3.5 × 3.5 × 2.0mm^3; 57 interleaved axial slices and a GRAPPA acceleration factor of 2.

The scanning protocol also included acquisition of a high-resolution T1-weighted magnetization-prepared rapid acquisition with gradient multi echo (MPRAGE) imaging sequence with the following acquisition parameters: TR = 2200ms; TE = 1.54, 3.36, 5.18, and 7ms; FOV = 230mm; voxel dimensions = 1.2 × 1.2 × 1.2mm^3; 144 slices.

fMRI preprocessing

Images were preprocessed and analyzed using Statistical Parametric Mapping software (SPM12; http://www.fil.ion.ucl.ac.uk/spm). Raw images were first visually inspected for major artifacts and signal dropout. Next, functional data were realigned to the mean image of the series, slice-time corrected, and co-registered to the individual's structural image using the normalized mutual information approach. We used a unified segmentation approach for spatial normalization. Briefly, the co-registered structural image was segmented into different classes of tissue based on the tissue probability maps, bias corrected, and affine registered to the MNI152NLin64sym template (default in SPM). Finally, using the deformation field created in the prior step, the slice-time corrected functional images were spatially normalized to the MNI template using non-linear 4th degree B-spline interpolation, resampled to 2 × 2 × 2mm MNI template, and smoothed with a 4mm Gaussian kernel.

fMRI analysis

The first-level general linear model included six regressors (cue and outcome onsets during gain, loss and neutral trials). In addition, outcome onset times for rewards only (punishments were not analyzed for this study) were parametrically modulated by model-derived reward prediction error, and convolved with a hemodynamic response function. Covariates of no interest included

the cue and outcome during neutral trials, six motion realignment parameters, and a constant term that modelling the baseline of unchanged neural activity. Prediction error beta weights were extracted from anatomically-defined regions-of-interest in the left and right NAc, defined from the AAL atlas, which is publicly available as an SPM12 toolbox, http://www.gin.cnrs.fr/en/tools/aal/. A positive RPE beta value signified higher activation for unexpected reward and lower activation for unexpected omission of rewards during gain trials.

MRS acquisition and analysis

^{1}H-MRS acquisition used a modified protocol similar to that described in prior studies conducted at the McLean Imaging Center on a 3T Tim Trio Siemens scanner (16-18). Briefly, a 2 × 2 × 2cm voxel was placed in the mPFC, midsagittally, anterior to the genu of the corpus callosum. The voxel was first shimmed using a machine automated shimming routine, and additional manual shimming was performed as needed. A modified J-resolved protocol (2D-JPRESS), which has been found to show good test-retest reliability (19), was used. This sequence involved the collection of 22 TE-stepped spectra with an echo time ranging from 35ms to 250ms in 15ms increments (TR = 2s, f1 acquisition bandwidth = 67Hz, spectral bandwidth = 2kHz, readout duration = 512ms, NEX = 16/TE-step, approximate scan duration = 12min) providing enough J-resolved bandwidth (67Hz) to resolve glutamate and glutamine.

To quantify glutamate and glutamine with the JPRESS data, the 22 TE-stepped free-induction decay series (FIDS) was zero-filled out to 64 points, Gaussian-filtered, and Fourier-Transformed using GAMMA-simulated J-resolved basis sets modeled for 2.89 T. Every J-resolved spectral extraction within a bandwidth of 67Hz was fit with the spectral-fitting package LCModel (20) and its theoretically-correct template. The integrated area under the entire 2D surface for each metabolite was calculated by summing the raw peak areas across all 64 J-resolved extractions for each metabolite as in prior publications (16, 17, 21). In this study, our primary outcome of ^{1}H-MRS measurements was the ratio of glutamine to glutamate (Gln/Glu).

Supplemental Results

Differences in reward learning and associated circuitry as a function of mood disorder polarity

Mean reward learning, ΔRewP, NAc RPE and mPFC Gln/Glu in the healthy control, unipolar-presenting and bipolar-presenting groups are shown in Figure S2. In terms of behavioral reward learning, a main effect of *Block* emerged from the *Group* (control, unipolar, bipolar) x *Block* (1,2,3) ANOVA for PRT response bias, $F(2,218)=4.11$, $p=0.02$, $\eta_p^2=0.04$. Bonferroni-corrected post hoc tests showed that response bias was significantly higher in block 3 than in block 1 ($p=0.03$), indicating that the asymmetrical reinforcement ratio was effective at inducing a behavioral response bias across the sample. However, neither the main effect of *Group*, nor the *Group* x *Block* interaction was significant (both ps>0.05), indicating that response bias did not significantly differ across control, unipolar and bipolar groups.

Similarly, the main effect of *Group* was not significant for the ΔRewP, $F(2,88)=0.45$, $p=0.64$, $\eta_p^2=0.01$ or mPFC Gln/Glu ratio, $F(2,99)=1.07$, $p=0.35$, $\eta_p^2=0.02$. Likewise, no main effects or interactions emerged from the *Group* x *Hemisphere* ANOVA for NAc RPE (all ps>0.05).

Bivariate associations between ΔRewP, NAc RPE and mPFC Gln/Glu, and symptom severity

Although the primary aim of the study was to conduct a multimodal investigation of the links between reward learning neurocircuitry and mood symptoms, we also conducted exploratory bivariate analyses to determine whether each of the neural markers, when examined individually, was associated with baseline anhedonic, (hypo)manic and impulsive symptom severity. To ensure consistency with the multimodal regression models reported in the main manuscript, we controlled for age, sex and medication load, and restricted analyses to the two patient groups.

When examined individually (rather than in a multimodal model) the ΔRewP was correlated with anhedonia severity on the MASQ-AD subscale, such that blunted ΔRewP amplitude was associated with more severe baseline anhedonia across the two patient groups (partial $r=-0.26$, $p=0.04$). Furthermore, and consistent with the results of our multimodal analysis, increased mPFC Gln/Glu was associated with greater baseline (hypo)manic symptom severity on the BISS-mania subscale for individuals in the bipolar group only (partial $r=0.51$, $p=0.04$).

Supplemental Discussion

Reasons for the lack of differences in the units of analysis between categorically-defined mood disorder subgroups

As shown in Figure S2, although we observed slight potentiation of reward learning and NAc RPEs in the bipolar group, we did not observe any significant differences between the three groups (when categorically-defined) on any of the units of analysis. This contrasts with the findings from prior studies that have found evidence of blunted reward learning on the PRT, RewP amplitude, NAc RPEs and mPFC Gln/Glu in individuals with a diagnosis of MDD, and potentiation of these effects in individuals with a diagnosis of BD (see Introduction of the main manuscript for an overview).

In contrast to the majority of prior studies examining categorical group differences in these units of analysis between controls and patients with mood disorders, we adopted a substantially more inclusive selection criteria with regards to comorbidity, substance use, medication and current mood state. Accordingly, our sample comprised a heterogeneous group of patients with multiple comorbidities who presented with depressed, mixed, and hypomanic episodes, or who were in partial remission from a mood episode. Furthermore, participants were recruited so that their performance on a behavioral measure of reward learning spanned a normative distribution. This means that our study sampled the entire range of individuals, spanning patients with mood disorders who had normative reward learning, those who had a unipolar mood disorder but potentiated reward learning, as well as individuals with a bipolar mood disorder who had blunted reward learning. This approach is in line with the RDoC framework, which remains agnostic to diagnosis and recognises that mental illness can be considered as falling along multiple dimensions, with traits that exist on a continuum from normal to extreme.

The absence of clear differences between categorically-defined diagnostic groups in our study shows that in diverse, clinically heterogeneous and comorbid samples (which are the norm rather than the exception in clinical practice), diagnostic categories fail to capture differences in underlying neurobiology – a finding that echoes a central tenet of the RDoC initiative.

Implications of sample size and adjustment for multiple comparisons

The current study is one of the first to simultaneously test three discrete biomarkers of reward learning neurocircuitry as predictors of mood disorder symptom severity and trajectory.

However, due to the resource-intensive nature of the study, we were limited in terms of overall sample size. This has important implications for reproducibility and generalizability, which need to be addressed in future studies using larger samples. For example, although our analyses were defined *a priori*, the significant correlations among the different units of analysis reported in Table S1 would not survive correction for multiple comparison. Furthermore, the reliability of model estimates in the bipolar group (particularly for the longitudinal analyses) should be interpreted with caution given the small size of the bipolar sample. Accordingly, we emphasize that the findings should be considered preliminary, and must be replicated in order to determine their robustness.

Supplemental References

1. Folstein MF, Folstein SE, McHugh PR (1975). "Mini-mental state": a practical method for grading the cognitive state of patients for the clinician. *J Psychiatric Res* 12: 189-98.
2. Pizzagalli DA, Jahn AL, O'Shea JP (2005). Toward an objective characterization of an anhedonic phenotype: a signal-detection approach. *Biol Psychiatry* 2005; 57: 319-27.
3. First MB, Spitzer RL, Gibbon M, Williams JB (2002). *Structured Clinical Interview for DSM-IV-TR Axis I Disorders, Research Version, Patient Edition (SCID-I/P)*. Biometrics Research, New York State Psychiatric Institute: New York, NY.
4. Watson D, Weber K, Assenheimer JS, Clark LA, Strauss ME, McCormick RA (1995). Testing a tripartite model: I. Evaluating the convergent and discriminant validity of anxiety and depression symptom scales. *J Abnorm Psychol* 104: 3-14.
5. Beck AT, Steer RA, Brown GK (1996). *Beck depression inventory-II: Manual*. Psychological Corp: San Antonio, TX.
6. Young RC, Biggs JT, Ziegler VE, Meyer DA (1978). A rating scale for mania: reliability, validity and sensitivity. *Br J Psychiatry* 133: 429-35.
7. Gonzalez JM, Bowden CL, Katz MM, Thompson P, Singh V, Prihoda TJ, et al (2008). Development of the Bipolar Inventory of Symptoms Scale: concurrent validity, discriminant validity and retest reliability. *Int J Meth Psych Res* 17: 198-209.
8. Patton JH, Stanford MS, Barratt ES (1995). Factor structure of the Barratt impulsiveness scale. *J Clin Psychol* 51: 768-74.
9. Sackeim HA (2001). The definition and meaning of treatment-resistant depression. *J Clin Psychiatry* 62: S1-S17.
10. Keller MB, Lavori PW, Friedman B, Nielsen E, Endicott J, McDonald-Scott P, et al (1987). The longitudinal interval follow-up evaluation: A comprehensive method for assessing outcome in prospective longitudinal studies. *Arch Gen Psychiatry* 44: 540-8.
11. Makeig S, Bell AJ, Jung T-P, Sejnowski TJ (eds.) (1996). Independent component analysis of electroencephalographic data. In: *Advances in Neural Information Processing Systems*, pp.145-151.
12. Perrin F, Pernier J, Bertnard O, Giard MH, Echallier JF (1987). Mapping of scalp potentials by surface spline interpolation. *Electroencephalogr Clin Neurophysiol* 66: 75-81.
13. Pascual-Marqui RD (2002). Standardized low-resolution brain electromagnetic tomography (sLORETA): technical details. *Methods Find Exp Clin Pharmacol* 24 (Suppl D): 5-12.
14. Pessiglione M, Seymour B, Flandin G, Dolan RJ, Frith CD (2006). Dopamine-dependent prediction errors underpin reward-seeking behaviour in humans. *Nature* 442: 1042-1045.
15. Sutton RS, Barto AG (1998). *Introduction to Reinforcement Learning*. MIT Press: Cambridge, MA.

16. Brennan BP, Hudson JI, Jensen JE, McCarthy J, Roberts JL, Prescot AP, et al (2010). Rapid enhancement of glutamatergic neurotransmission in bipolar depression following treatment with riluzole. *Neuropsychopharmacology* 35: 834-46.

17. Brennan BP, Jensen JE, Perriello C, Pope Jr HG, Jenike MA, Hudson JI, et al (2016). Lower posterior cingulate cortex glutathione levels in obsessive-compulsive disorder. *Biol Psychiatry Cogn Neurosci Neuroimaging* 1: 116-24.

18. Brennan BP, Tkachenko O, Schwab ZJ, Juelich RJ, Ryan EM, Athey AJ, et al (2015). An examination of rostral anterior cingulate cortex function and neurochemistry in obsessive–compulsive disorder. *Neuropsychopharmacology* 40: 1866-76.

19. Jensen JE, Auerbach RP, Pisoni A, Pizzagalli DA (2017). Localized MRS reliability of in vivo glutamate at 3 T in shortened scan times: a feasibility study. *NMR Biomed* 30: e3771.

20. Provencher SW (1993). Estimation of metabolite concentrations from localized in vivo proton NMR spectra. *Magn Reson Med* 30: 672-9.

21. Jensen JE, Licata SC, Öngür D, Friedman SD, Prescot AP, Henry ME, et al (2009). Quantification of J-resolved proton spectra in two-dimensions with LCModel using GAMMA-simulated basis sets at 4 Tesla. *NMR Biomed* 22: 762-9.

Figure S1. Participant flow diagram

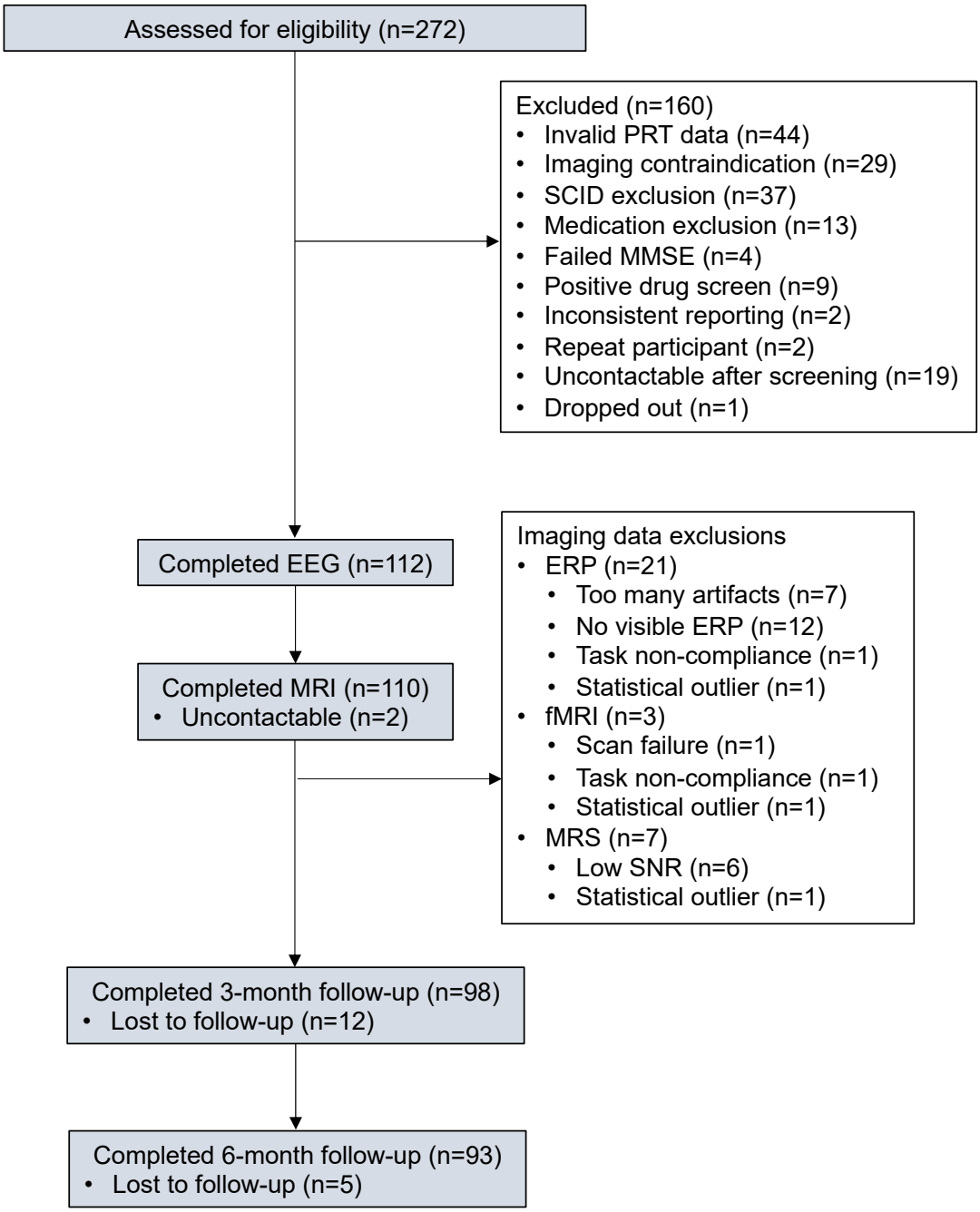

Figure S1. Figure shows the flow of participants into the study from screening to 6-month follow-up, along with reasons for exclusion from imaging sessions and from analysis.
PRT=Probabilistic Reward Task; SCID=Structured Clinical Interview for DSM-IV; MMSE=Mini Mental State Exam; EEG=electroencephalography; ERP=event-related potential; fMRI=functional magnetic resonance imaging; MRS=magnetic resonance spectroscopy; SNR=signal-to-noise ratio.

Figure S2. Reward learning units of analysis across diagnostic categories

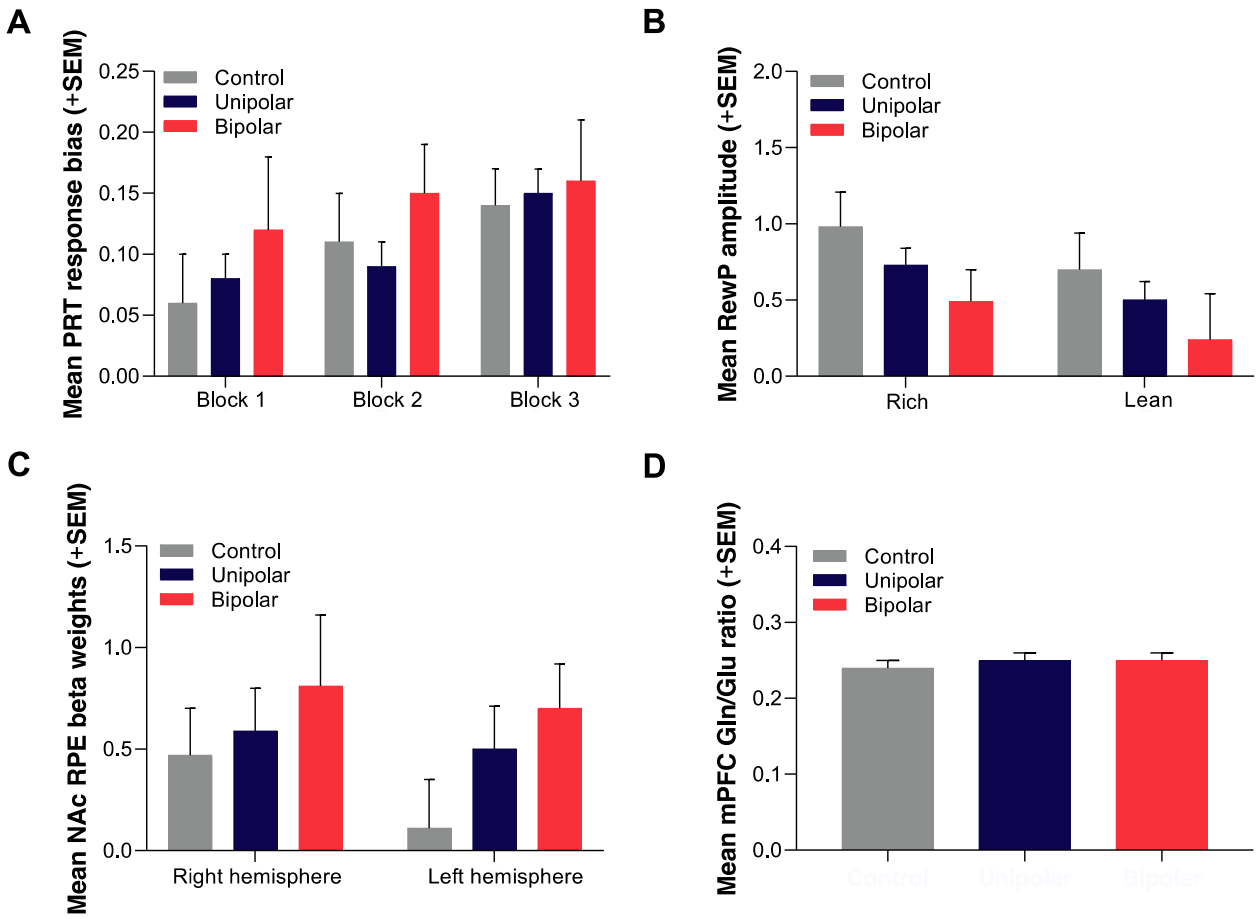

Figure S2. Figure shows the raw mean (+ standard error of the mean; SEM) (**A**) reward learning (i.e., response bias in blocks 1, 2, and 3 of the Probabilistic Reward Task; PRT), (**B**) Reward positivity (RewP) component amplitude in response to rewards following rich and lean trials on the PRT, (**C**) reward prediction error beta weights from the left and right nucleus accumbens, and (**D**) the ratio of glutamine to glutamate (Gln/Glu) in the medial prefrontal cortex (mPFC), across the healthy control (grey bars), unipolar mood disorders (blue bars) and bipolar mood disorders (red bars) groups.

Figure S3. Associations between neural markers and behavioral reward learning

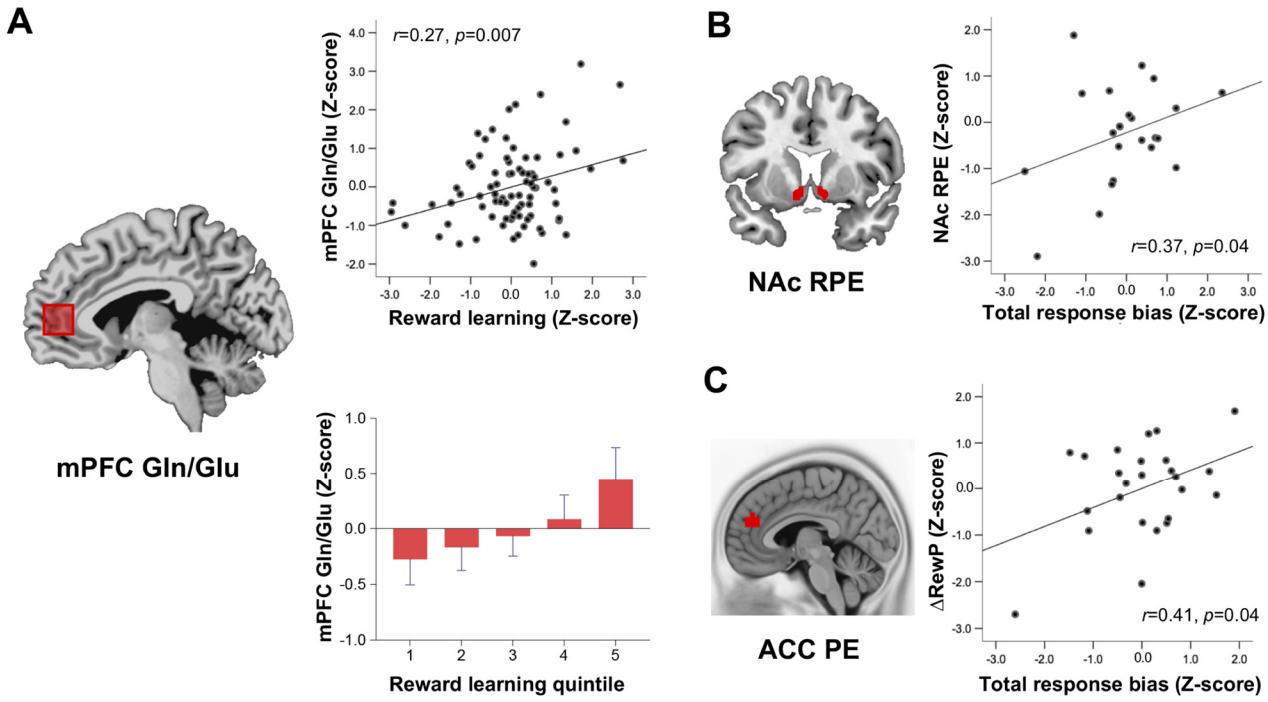

Figure S3. Panel **A** shows associations between behavioral reward learning on the Probabilistic Reward Task (PRT) and medial prefrontal cortex glutamine to glutamate ratio (mPFC Gln/Glu). Scatterplot shows a positive correlation between greater reward learning and higher levels of mPFC Gln/Glu (r=0.27, p=0.007). This correlation is consistent with the linear increase in mPFC Gln/Glu observed across the five reward learning quintiles (bars show mean standardized mPFC Gln/Glu + standard error). Although the nucleus accumbens reward prediction error signals (NAc RPE) and anterior cingulate cortex prediction error signals (ACC PE; defined as the delta reward positivity amplitude; ΔRewP) were not correlated with our *a priori*-defined learning measure (block 3 minus block 1 response bias), they did correlate with a separate aspect of learning on this task – total response bias – in the healthy control group. Scatterplot in Panel **B** shows a positive correlation between stronger NAc RPE signals and higher total response bias in the healthy control group (r=0.34, p=0.04). Scatterplot in Panel **C** shows a positive correlation between stronger RewP amplitude and greater total response bias in the healthy control group (r=0.41, p=0.04). All values plotted represent standardized (Z) scores.

Figure S4. Neural markers and symptoms across the reward learning quintiles

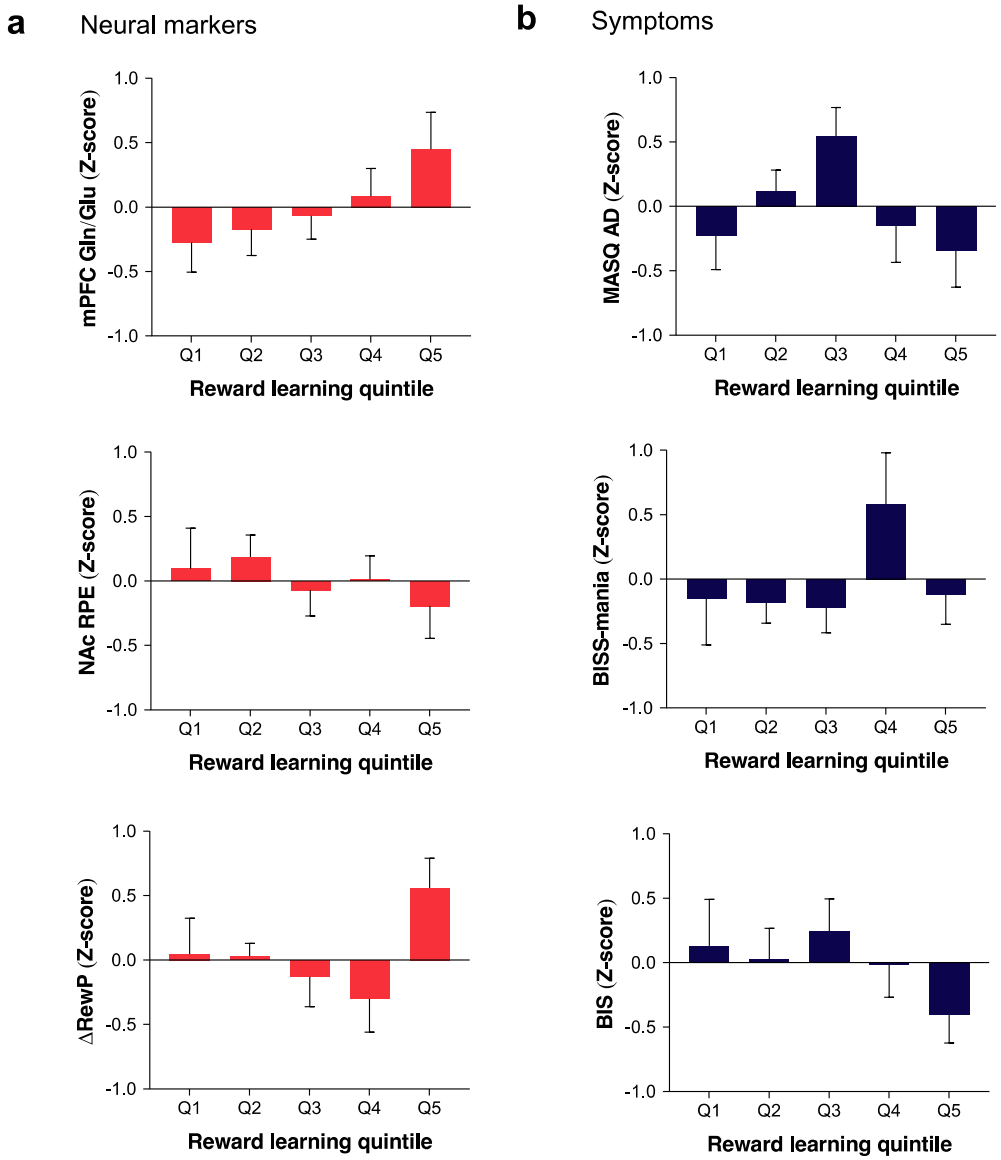

Figure S4. Figures in Panel **A** show variation in medial prefrontal cortex glutamate (mPFC Gln/Glu; top figure), nucleus accumbens reward prediction error signals (NAc RPE; middle figure), and anterior cingulate cortex prediction error signals/reward positivity amplitude (ΔRewP; bottom figure), across the reward learning quintiles for the whole sample. Figures in Panel **B** show variation in anhedonia on the Anhedonic Depression subscale of the Mood and Anxiety symptom Questionnaire (MASQ-AD; top figure), (hypo)mania on the Mania subscale of the Bipolar Inventory of Symptoms Scale (BISS-mania; middle figure) and impulsivity on the Barratt Impulsiveness Scale (BIS; bottom figure) across the reward learning quintiles in the patients. Scores on each measure are standardized (Z-scores derived using the mean and standard deviation from the whole sample for neural markers and the patients only for symptoms) and bars represent the mean + standard error of the mean. Individuals in higher quintiles were those who showed greater increases in response bias from the first to the last block of the Probabilistic Reward Task.

Figure S5. Changes in symptoms across time in the patient groups

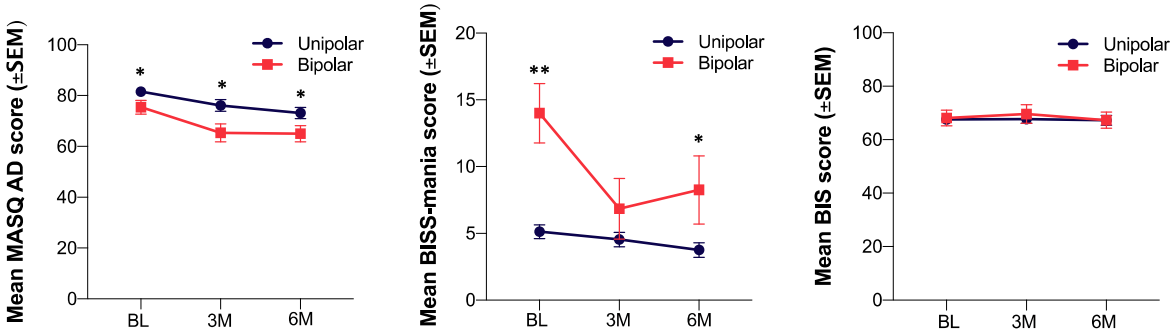

Figure S5. Figures show changes in anhedonic symptom severity on the Anhedonic Depression subscale of the Mood and Anxiety Symptom Questionnaire (MASQ-AD), (hypo)manic symptom severity on the mania subscale of the Bipolar Inventory of Symptoms Scale (BISS-mania), and impulsivity on the Barratt Impulsiveness Scale (BIS) from baseline (BL) to 3-month follow-up (3M) and 6-month follow-up (6M) in the unipolar and bipolar mood disorder groups. Points plotted represent the raw mean score on each scale ± standard error of the mean. Asterisks indicate significant group differences at each time point. *p<0.05; **p<0.001

Table S1. Correlations between neural indices and behavioral reward learning across the whole sample, and in the healthy control, unipolar and bipolar mood groups separately

	ΔRewP	NAc RPE	mPFC Gln/Glu
Whole sample			
Overall learning	0.16 (0.14)	0.12 (0.21)	0.01 (0.89)
Slope of learning	0.03 (0.77)	-0.18 (0.07)	**0.27** (0.007)**
Control group			
Overall learning	**0.41* (0.04)**	**0.37* (0.04)**	0.08 (0.67)
Slope of learning	0.04 (0.86)	-0.23 (0.21)	0.17 (0.38)
Unipolar group			
Overall learning	-0.05 (0.75)	-0.13 (0.36)	-0.12 (0.38)
Slope of learning	-0.10 (0.51)	-0.15 (0.27)	**0.40** (0.003)**
Bipolar group			
Overall learning	0.24 (0.38)	0.36 (0.14)	0.20 (0.42)
Slope of learning	0.32 (0.23)	-0.24 (0.32)	0.19 (0.45)

*No*te. Values shown are Pearson's r values with p values indicated in parentheses. Correlations between learning and NAc RPE and mPFC Gln/Glu use learning values from the PRT that was performed behaviorally at the first screening session. Correlations between learning and ΔRewP were computed using learning values from the alternate version of the PRT that was performed during EEG recording.
*p<0.05; **p<0.01.

Table S2. Correlations among the neural indices in the whole sample, healthy control, unipolar, and bipolar mood groups separately.

	NAc RPE	mPFC Gln/Glu
Whole sample		
ΔRewP	-0.07 (0.52)	0.04 (0.74)
NAc RPE		0.06 (0.50)
Control group		
ΔRewP	-0.15 (0.46)	0.13 (0.55)
NAc RPE		0.11 (0.58)
Unipolar group		
ΔRewP	0.06 (0.67)	-0.04 (0.77)
NAc RPE		0.03 (0.81)
Bipolar group		
ΔRewP	-0.44 (0.12)	-0.06 (0.85)
NAc RPE		0.01 (0.97)

Note. Values shown are Pearson's r values with p values indicated in parentheses.

Table S3. Regression model testing whether mPFC Gln/Glu explains a greater proportion of longitudinal (hypo)manic symptom severity relative to behavioral reward learning alone

Dependent variable: 3-month (hypo)manic symptom severity

	B	SE	β	*T*	*p*
Model 1					
(constant)	0.06	2.02		0.03	0.98
Age	0.09	0.06	0.19	1.60	0.11
Sex	-0.83	1.23	-0.08	-0.68	0.50
Medication load	-0.02	0.32	-0.01	-0.08	0.94
Baseline BISS-mania	0.41	0.10	0.60	3.94	<0.001
Group	-2.68	1.58	-0.26	-1.70	0.10
Reward learning	-4.00	2.96	-0.22	-1.35	0.18
Group x Reward learning	3.42	4.31	0.13	0.79	0.43
Model 2					
(constant)	1.73	2.11		0.82	0.42
Age	0.06	0.06	0.13	1.02	0.31
Sex	-2.28	1.29	-0.23	-1.77	0.08
Medication load	-0.14	0.31	-0.06	-0.46	0.65
Baseline BISS-mania	0.36	0.10	0.52	3.55	0.001
Group	-1.73	1.55	-0.17	-1.12	0.27
Reward learning	-1.56	3.08	-0.09	-0.51	0.61
Group x Reward learning	0.08	4.32	0.00	0.02	0.99
mPFC Gln/Glu	-20.53	14.17	-0.22	-1.45	0.15
Group x mPFC Gln/Glu	70.95	25.40	0.43	2.79	0.007

Model Summary

Model	R	R^2	Adjusted R^2	SE of estimate	R^2 change	F change	df1	df2	Sig. F change
1	0.53	0.28	0.19	4.20	0.28	3.08	7	55	0.008
2	0.61	0.37	0.27	4.00	0.09	3.91	2	53	0.026

Note. Group was dummy-coded 0=unipolar, 1=bipolar; BISS-Mania=Bipolar Inventory of Symptoms Scale mania subscale score; RewP=reward positivity; NAc RPE=nucleus accumbens reward prediction error; mPFC Gln/Glu=medial prefrontal cortex ratio of glutamine to glutamate.